Measuring $V_{\rm tb}$ and the Polarization of Top Quarks and W Bosons via Boson Gluon Fusion at ATLAS

Beatriz González Piñeiro [1], Dugan O'Neil [2],
Raymond Brock [1] and Michel Lefebvre [2]

1 Michigan State University
2 University of Victoria

Abstract

The production of single top quarks via the electroweak interaction promises to provide new opportunities to both test the Standard Model and search for new physics. In particular, electroweak top production provides the only means to directly measure the CKM matrix element $V_{\rm tb}$ and provides the only source of highly polarized top quarks at ATLAS. These processes also allow measurements related to the decay properties of the top quark which are independent from those performed via $\rm t\bar{t}$ production.

Boson gluon fusion is the highest rate mechanism of electroweak top production leading to electroweak top measurements with the highest statistical precision. In addition this channel benefits from a good signal to background ratio. With these features, boson gluon fusion provides an optimal environment to measure $V_{\rm tb}$, top quark polarizations and properties of the W-t-b vertex.

A measurement of $V_{\rm tb}$ in this channel is presented. It is found that $V_{\rm tb}$ can be measured via boson gluon fusion with a statistical precision of 0.27% after 3 years of low luminosity data taking ($3\times10^4 \rm pb^{-1}$) at the LHC. The potential of ATLAS to measure the top quark polarization and the helicity of the W boson in this channel is also presented. A precision of a few percent is expected in these measurements. The precision which can be reached sets the limit of sensitivity to non Standard Model effects.

1 Introduction

To date the only observed mechanism for top quark production is $t\bar{t}$ pair-production via the strong interaction. The production of single top quarks via electroweak interactions has yet to be observed, but promises new opportunities to both test the Standard Model and search for new physics. Single top quark processes provide a unique opportunity to perform a direct measurement of the CKM matrix element V_{tb}, and to test the Standard Model prediction for the polarization of the top quark and its decay products.

There are three major diagrams for single top quark production at the LHC. These diagrams are shown in Figure 1 along with their major backgrounds. The dominant single top quark mechanism is boson gluon fusion (Wg), followed according to rate by Wt, and then by s-channel (W^*) production. With respect to other single top quark channels, the primary advantage of boson gluon fusion is the high rate, leading to a high statistical precision in this channel. This process contributes about 70% of the total single top quark cross-section at LHC. A detailed discussion of cross-sections will be presented in Section 2.

The value of the CKM matrix element V_{tb} has never been directly measured. Despite this fact it is, as a fraction of its value, the most highly constrained element of the matrix [1, 2]. This deduction relies on a unitarity constraint which assumes three quark generations (ie. $|V_{td}|^2 + |V_{ts}|^2 + |V_{tb}|^2 = 1$). If this assumption is invalid the value of V_{tb} is virtually unconstrained. A measurement of V_{tb} different from the predicted value would imply the existence of physics beyond the Standard Model. For example, the existence of flavour-changing neutral currents could modify the rate of Wg events and hence change the measured value of V_{tb} in this channel.

There are several ways to obtain indirect information on V_{tb}. The dominant mechanism for producing top quarks at the LHC is $t\bar{t}$ production. Although this source of top quarks contains two W-t-b vertices in its decay, it cannot be used to make a direct measurement of V_{tb}. Measurements from $t\bar{t}$ production have been used to constrain V_{tb} only in a 3-generation model (see the CDF measurement [3]). V_{tb} can also be constrained by comparing precision electroweak measurements to loop corrections containing the W-t-b vertex. Electroweak top quark production is the only way to produce a direct measurement of V_{tb} at a hadron collider. Each single top quark process has a cross-section which is directly proportional to $|V_{tb}|^2$. By measuring the rate of single top quark processes and combining this information with the value of the $t \to Wb$ branching ratio and top quark mass measurements from the $t\bar{t}$ channel, the absolute value of V_{tb} can be extracted.

Top quark polarization is also precisely predicted in the Standard Model. Top quarks produced via the dominant $t\bar{t}$ process are, to first order, unpolarized. Higher order diagrams will induce some polarization in the $t\bar{t}$ sample at the LHC but the effects are predicted to be small [4]. Event-by-event spin correlations of top quarks in $t\bar{t}$ production

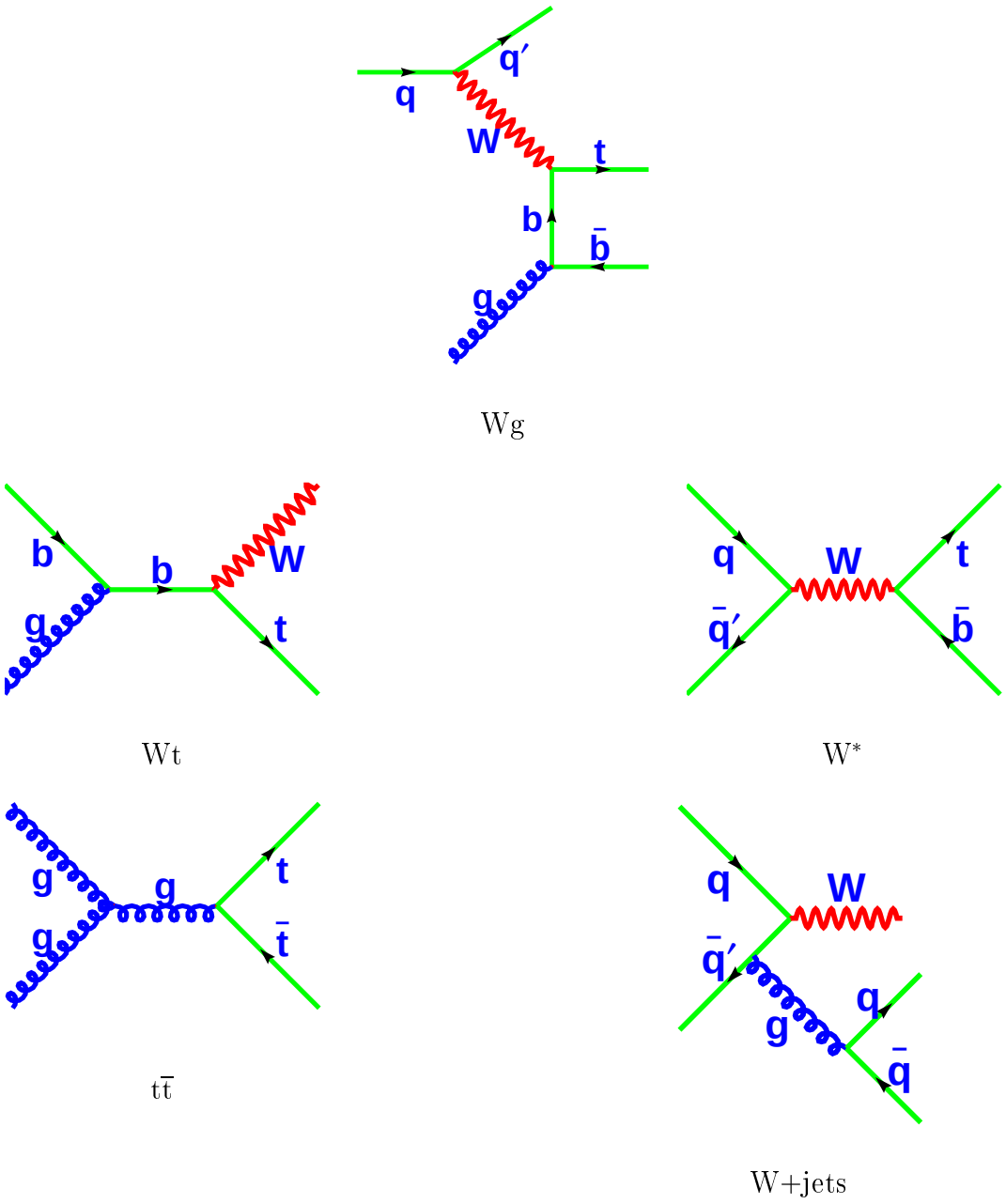

Figure 1: *Single top quark signals and backgrounds at LHC. Reading from left to right, top to bottom the diagrams are W-g fusion, Wt, W*, and backgrounds* $t\bar{t}$ *and W+jets.*

could be observable by ATLAS, as suggested in references [4, 5]. Fortunately, electroweak top quark processes are a source of highly polarized top quarks and since the top quark decays before it can hadronize, the polarization present in its production is transmitted to its decay products. From the study of the angular distribution of the charged lepton emitted in W boson decay it will be possible to separately characterize the polarization of the top quark and the W boson involved in the process. Deviations from the predicted behaviour, such as right handed couplings, or an unexpected mixture of the left handed and longitudinal components for the W boson, could be a sign of new physics.

This note explores the possibilities offered by the boson gluon fusion single top quark production channel to test the predictions of the Standard Model about the value of V_{tb} and the polarizations of the top quark and W boson.

Section 2 presents the cross-sections of the Wg signal and main backgrounds expected at the LHC. Section 3 discusses the Monte Carlo generators used for each process and the overall cross-section normalization applied to each signal. Section 4 focuses on kinematic distributions of signal and background and describes the event selection strategy. Section 5 treats the results expected in a V_{tb} measurement obtained via Wg fusion. Section 6 discusses the possibilities of measuring top quark and W boson polarization via boson gluon fusion. Finally, Section 7 presents the conclusions.

2 Cross-sections

The cross-sections assumed for the main signals and backgrounds are presented in Table 1 for 175 GeV/c^2 top quarks. This table illustrates the size of the backgrounds relative to the Wg signal. The Wg fusion, W* and $\mathrm{t\bar{t}}$ cross-sections come from analytic, next-to-leading order calculations. The cross-sections for Wt, W+jets and $\mathrm{Wb\bar{b}}$ come from Monte Carlo calculations with leading-order matrix elements.The column of $\sigma\times$BR includes only top quark decays to electrons and muons as these are the final states considered in this study.

The Wg process is the largest source of top quarks via electroweak production at the LHC, with a rate which is almost 1/3 of the rate of $\mathrm{t\bar{t}}$ production. Due to the high cross-section predicted, this process is expected to be a good source of physics information. However, it must also be noted that the Wg cross-section calculation relies on gluon parton density functions (pdf) and the errors due to pdf uncertainties are potentially significant. Table 2 shows the sources and levels of theoretical error in Wg-fusion and s-channel single top quark production. The s-channel process, which suffers from a low rate in comparison with Wg, is less affected by the theoretical errors. These processes provide two independent measurements of V_{tb} subject to different sources of error. The total uncertainty on both measurements will be comparable. A mesurement of V_{tb} via s-channel events at the LHC has been presented in reference [13]. However, polarization studies using the s-channel process, will suffer from a lack of statistics.

process	generator	total cross-section (pb)	$\sigma\times$ BR (pb)
Wg-fusion	ONETOP	244 [6]	54.2
Wt	ONETOP	60	17.8
W^*	ONETOP	10 [7]	2.22
$t\bar{t}$	ONETOP	830 [8]	246
$Wb\bar{b}$	M.E + HERWIG	300 [9]	66.7
W+jets	HERWIG	18000	4000

Table 1: *Cross-sections for the processes considered in this study and the cross-section $\times$ branching ratio relevant to the study of only electron and muon final states. The cross-section for the W+jets process is obtained by normalizing the cross-section obtained from HERWIG [10] with cuts requiring at least 2 jets above 15 GeV with $|\eta| < 3.2$ to the cross-section from VECBOS [11] for these cuts. HERWIG is then used to estimate the cross-section when the jet region is extended to $|\eta| < 5$ in order to obtain 18000 pb. The generator for the $Wb\bar{b}$ process is the combination of a matrix element from [12] and HERWIG.*

Source	W^*	Wg
pdf	4%	10%
μ (scale)	4%	4%
ΔM_t	5%	2%

Table 2: *Sources and levels of theoretical error in the cross-sections of Wg and W^*. The error due to imprecision in the mass of the top quark is calculated assuming the mass is known to 2 GeV (expected from LHC measurements). In this table pdf refers to the error calculated by choosing different parton density function sets. The μ (scale) refers to the error obtained by varying the renormalization scale at which the calculation is performed [14]. The error in the gluon pdf is from [15], all other numbers are taken from [16].*

3 Generators

In this study all of the processes containing top quarks were generated using the ONETOP [17] generator. This is a parton-level leading-order generator which keeps all helicity information and hence produces the correct angular distributions of top quark decay products. The particles from ONETOP were then passed to PYTHIA [18] which fragmented the final state particles, added initial and final state radiation and simulated the underlying event. Finally events were passed into ATLFAST [19] version 1.61 in order to apply ATLAS-like detector smearing effects.

The non-top quark backgrounds considered in this study were generated using HERWIG [10] and were also passed through ATLFAST version 1.61. The $Wb\bar{b}$ background was generated using non-standard HERWIG code which interfaces the $Wb\bar{b}$ matrix element from [12] to HERWIG. The W+jets process is a standard HERWIG process. Since the quark jets in the W+jets process are assumed to be massless, the cross-section for this process becomes infinite at low jet transverse momentum (collinear divergence). To avoid this problem the cross-section for this process was defined only when 2 jets above 15 GeV P_{T} were found within $|\eta| < 5$ using the standard ATLFAST cone-based jet finding algorithm (R=0.4). The cross-section has been normalized using the value from the VECBOS [11] Monte Carlo generator.

4 Event selection

In order to understand the differences between the Wg signal and its major backgrounds it is necessary to compare a variety of kinematic variables. Distributions of several useful variables are presented in this section. Each distribution has been normalized to unit area in order to emphasize kinematic rather than rate differences. All of the plots displayed herein are created after ATLFAST and ATLFAST-B[1] have been used to smear the distributions. So, all observables must meet their default definitions in ATLFAST. In ATLFAST-1.61 these defaults for electrons, jets and b-jets are:

- isolated electrons: $|\eta| < 2.5, P_{\mathrm{T}} > 5$ GeV, separation of $R > 0.4$ from other clusters and $E_{\mathrm{T}}<$ 10 GeV in an R =0.2 cone, where $R = \sqrt{(\Delta\eta)^2 + (\Delta\phi)^2}$
- jet: $|\eta| < 5, P_{\mathrm{T}} > 15$ GeV;
- b-jet: jet and $|\eta| < 2.5$, 60% tagging efficiency, 10% charm-mistag rate and 1% light-quark mistag rate. b-jets were tagged without p_T dependence.

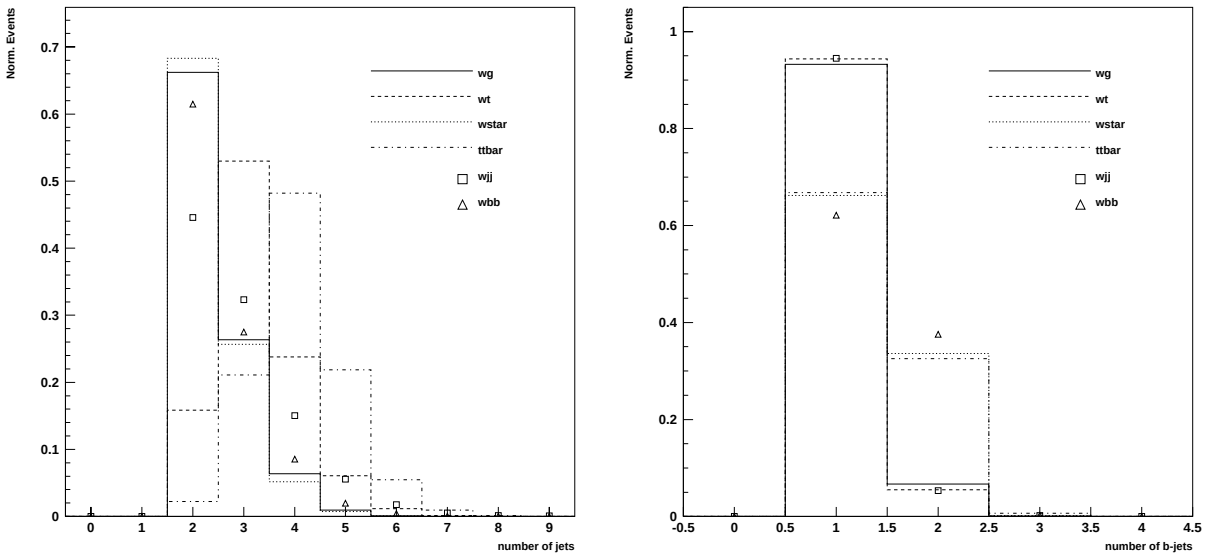

Figure 2: *The number of jets (left) and b-jets (right) found in signal and background after ATLFAST and ATLFAST-B. Refer to text for a description of the event selection.*

Trigger-level cuts have also been applied before the distributions in this section were created. These cuts should mimic the effect of a single top quark trigger selection. The cuts used are:

- at least 1 lepton above 20 GeV P_{T};
- at least 1 b-jet above 50 GeV P_{T};
- at least 1 other jet above 30 GeV P_{T}.

The trigger efficiency associated with these cuts is presented in Table 3. This pre-selection reduces the total non-top quark background by about a factor of 10^2. Note that the trigger is efficient for both, single top quark production and top quark pair production. Therefore, the presence of two top quark decays results in half of the percentage reduction of top quark events for pair production as for the signal single top quark events.

The first variable of interest is the number of jets in the event. Figure 2 shows the number of reconstructed jets in an event for the Wg signal and each of its backgrounds. These distributions illustrate that, on average $\mathrm{t\bar{t}}$, as well as Wt events, produce more jets than Wg events. In fact, a cut requiring the presence of exactly 2 jets in each event is a major

[1] ATLFAST-B is a set of routines to simulate efficiencies for tagging b-jets, tau-jets and c-jets. These routines also provide jet-energy calibration.

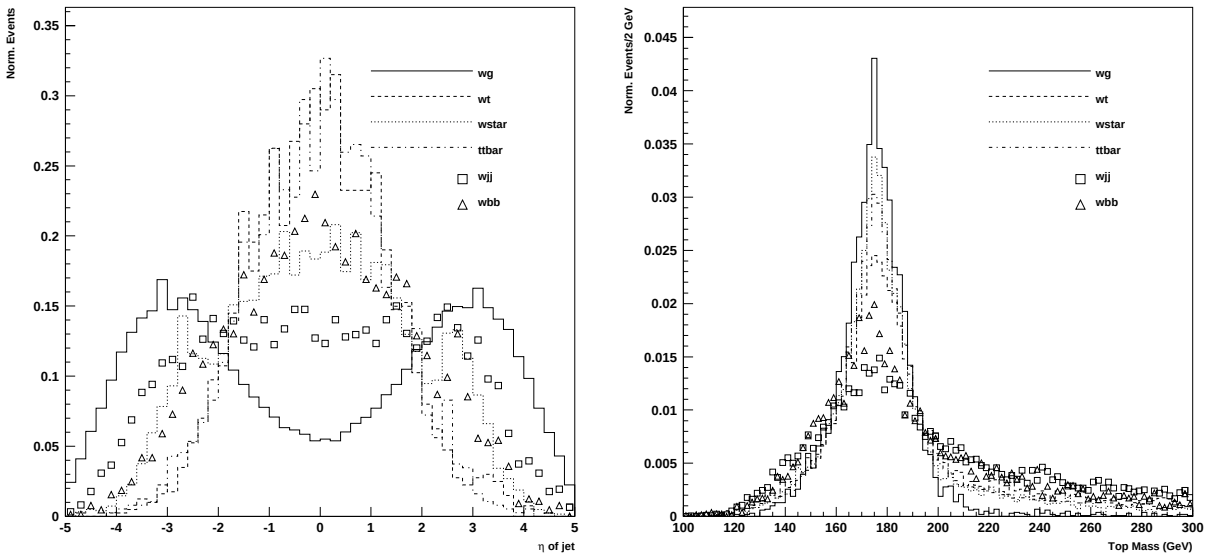

Figure 3: *Left: Eta distribution of non b-tagged jets. Right: Invariant mass of the l-b-ν combination that gives the best top quark mass. Refer to text for description of event selection.*

source of rejection of the $t\bar{t}$ background. The W+jets background will also be reduced by about one third when this cut is applied.

The second kinematic variable considered here is the number of b-jets tagged in an event, presented in Figure 2. As mentioned previously, in this sample of events there is already a requirement that there be at least one tagged b-jet (hence the absence of events in the zero-jet bin). Although, in principle, Wg fusion events contain two b-jets, in practice one of the jets will quite often be missed (ie. not tagged) because it has low transverse momentum and will not meet the minimum b-tag requirements. It can be seen from this figure that requiring only one b-tagged jet will further enhance the Wg signal with respect to $t\bar{t}$.

An interesting feature of Wg fusion events, is the presence of a spectator quark jet in the forward direction. As illustrated in Figure 3, requiring a forward jet with $|\eta| > 2.5$ and P_{T}>50 GeV is an important cut to improve the signal over background ratio.

Another variable used to separate signal from background is the reconstructed top quark mass (since there is no top quark in the W+jets background). Figure 3 shows the top quark mass reconstructed by choosing the neutrino z-momentum which gives the best top quark mass. Since the only measure of the neutrino momentum is via the missing P_{T}, a W boson mass constraint is used to reconstruct the neutrino z-momentum within a 2-fold ambiguity. A choice of z-momentum must therefore be made in order to obtain the neutrino 4-vector. The solution corresponding to the best top quark mass has been found

cut	Wg fusion eff(%)	W* eff(%)	Wt eff(%)	$t\bar{t}$ eff(%)	$Wb\bar{b}$ eff(%)	W+jets eff (%)
trigger	18.3	27.0	25.5	43.4	2.53	0.663
njets=2	12.0	18.4	4.03	0.851	1.55	0.291
fwd jet $\|\eta\| > 2.5$	4.15	1.56	0.14	0.035	0.064	0.043
$M_{l\nu b}$ 150-200 GeV	3.00	0.72	0.064	0.017	0.023	0.016
events/ $3 \times 10^4 \mathrm{pb}^{-1}$ (before cuts)	1.63×10^6	66600	534000	7.2×10^6	2.0×10^6	12.0×10^7
events/ $3 \times 10^4 \mathrm{pb}^{-1}$ (after cuts)	48795 ± 40	482 ± 148	339 ± 21	1253 ± 228	464 ± 63	19018 ± 113

Table 3: *Cumulative effect of cuts on Wg signal and backgrounds. The upper part of this table refers to cumulative efficiencies of various cuts. The lower part refers to the number of events for* $3 \times 10^4 pb^{-1}$. *The branching ratio for W*$\rightarrow$ *e*ν *or* $\mu\nu$ *(2/9) has been applied in order to estimate the number of events corresponding to* $3 \times 10^4 pb^{-1}$. *Errors quoted in this table are purely statistical.*

to be right aproximately 70% of the time. An alternative choice was also considered, in which the solution selected the smallest value of the neutrino z-momentum. However, in this case the correct choice is made only 50% of the time.

Summarizing, in addition to the trigger selection described previously, the following set of cuts have been applied in order to separate signal and background:

- The total number of jets is equal to 2. Note than one jet is already tagged as a b-jet with $P_{\mathrm{T}} > 50$ GeV
- The second jet is not tagged, and is required to be in the forward region $|\eta| > 2.5$ with $P_{\mathrm{T}} > 50$ GeV
- The reconstructed top quark mass is in the window 150-200 GeV.

These cuts lead to the results presented in Table 3. This table lists the cumulative efficiency after applying each cut and the number of events expected after three years of LHC running at low luminosity ($3 \times 10^4 \mathrm{pb}^{-1}$). The errors quoted in the table are

estimated using the square root of the number of Monte Carlo events remaining after cuts. The results presented in this table correspond to a minimal set of cuts defined from a compromise between the necessity of a good signal to background ratio, and a good signal efficiency beneficial for increasing signal statistics in polarization measurements. Under this condition, the selections applied lead to a prediction for S/B of 2.3 and $S/\sqrt{B}$ of 332 (where S=signal and B=background). Introducing other event selection variables [4,20,21], it is possible to improve the signal to background ratio to nearly 5, but this does not improve the cross-section measurement due to the small remaining signal efficiency.

5 Measurement of $V_{\rm tb}$

Given existing measurements, the Standard Model provides precise predictions for the CKM matrix element $V_{\rm tb}$. Measuring the rate of electroweak top production provides the only way to do a direct measurement of $V_{\rm tb}$ at a hadron collider. The cross-section of Wg fusion is proportional to $|V_{\rm tb}|^2$, therefore, the precision in the production rate determines the precision in the measurement of $|V_{tb}|$.

The precision with which a cross-section can be measured is given by the fluctuation of the total number of events in the signal region, $S+B$. Hence, it would appear that the best strategy for the measurement of the cross-section is one which minimizes the ratio $\sqrt{S+B}/S$, the fractional uncertainty in the cross-section. However, because the error on the number of background will feed into the error on the cross-section, if the level of background is comparable to the level of signal (or greater) this strategy relies on good knowledge of the background cross-sections. In the case of W+jets and Wb$\overline{\rm b}$ production the cross-section at the LHC is not well known. For this reason, a different strategy has been adopted. This is to design event selection criteria as a compromise between the optimization of $\sqrt{S+B}/S$ and the optimization of the ratio S/B, allowing a reduction of the influence of the error on the W+jets and Wb$\overline{\rm b}$ cross-sections.

After applying the event selection presented in Section 4, which leads to the results presented in Table 3, the signal-to-background ratio expected for boson gluon fusion is 2.3. The statistical precision on the Wg fusion cross-section after three years (assuming an integrated luminosity of $3\times10^4{\rm pb}^{-1}$) is $\sqrt{S+B}/S = 0.54\%$. Since the cross-section is proportional to $|V_{\rm tb}|^2$, the statistical error expected on $V_{\rm tb}$ is 0.27%. The theoretical error affecting the Wg fusion cross-section is estimated to be 11% (see Table 2) The combination in quadrature of theoretical errors with the statistical error estimated above, yields a precision of $\Delta V_{\rm tb}/V_{\rm tb}$=5.5%. Clearly, the uncertainty of this measurement will be dominated by the theoretical and systematic errors, not statistics.

It is possible to perform a measurement of $V_{\rm tb}$ using other single top channels. The results for the W^* channel are presented in reference [13]. This channel suffers from a lower rate

but the theoretical errors are smaller, resulting in a precision of $\Delta V_{\rm tb}/V_{\rm tb}$=4.6%. Wg fusion and W^* provide two independent measurements of $V_{\rm tb}$, affected by different sources of error, leading to a similar precision. The two independent measurements serve as a cross-check, but they are also interesting individually as they are influenced differently by new physics [14].

6 Polarization

6.1 Introduction

The W-g fusion channel provides a sample of highly polarized top quarks. In addition this channel benefits from high statistics and a good signal-to-background ratio. With these advantages, Wg provides optimal conditions for the measurement of the polarization of the top quark.

In addition to being able to study the polarization induced by the electroweak top quark production vertex, it is possible to study the helicity of the W boson produced by the top quark decay. A top quark is expected to decay through a W-t-b vertex nearly 100% of the time. If the top quark is a spin 1/2 particle the ratio of right-handed to left-handed to longitudinal W's is precisely predicted by the Standard Model. Measuring this ratio probes the top quark decay vertex and is not sensitive to the polarization of the top quark itself. Hence this measurement can be cross-checked with the same measurement from the $t\bar{t}$ channel.

The sensitivity of the ATLAS experiment to both the polarization of the top quark and to the helicity of the W boson produced from its decay is presented in this section.

6.2 Angles and Frames

The measurements presented in this section involve angular distributions of top quark decay products. In order to make the measurements it is necessary to reconstruct three different reference frames and two different angles. Figure 4 illustrates the angles θ_l and ψ_l needed to make these measurements.

In order to measure the helicity of the W boson produced by the top quark decay the angle between the W boson direction in the top quark rest frame and the charged lepton direction in the W boson rest frame (ψ_l) is the only angle which needs to be reconstructed. For the measurement of top quark polarization the angle between the direction of the top quark in the center of mass frame of the incoming partons and the direction of the charged lepton in the top quark rest frame (θ_l) is the only angle which needs to be measured.

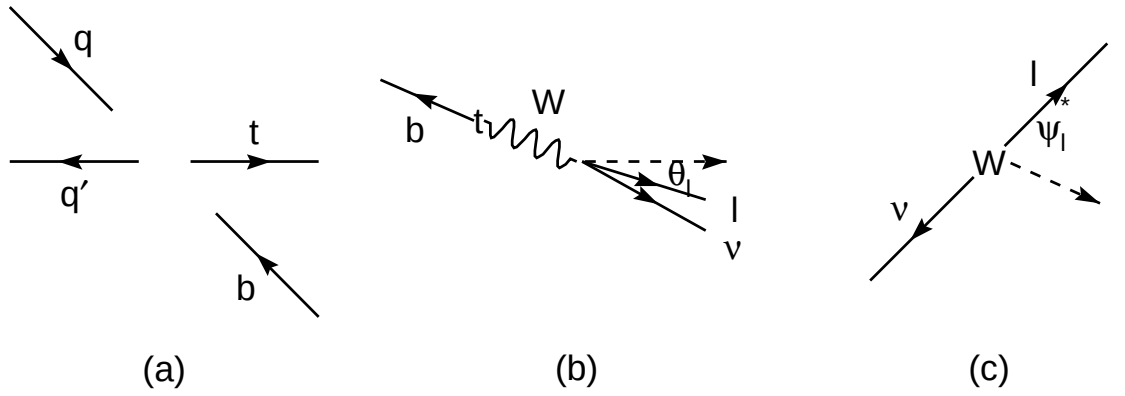

Figure 4: *Diagram of three frames used to measure top quark polarization and W boson helicity. (a) The center-of-mass of the incoming partons (q and b). The top quark and q′ are produced back-to-back in this frame. (b) The rest frame of the top quark. The W boson and the b quark are back to back in this frame. The dashed line represents the top quark direction in the center-of-mass of the incoming partons. θ_l is the angle between the top quark direction in the center-of-mass frame and the lepton direction in the top quark rest frame. (c) The rest frame of the W boson produced by top quark decay. The charged lepton and neutrino are back-to-back in this frame. The dashed line represents the W boson direction in the top quark rest frame. ψ_l is the angle between the W boson direction in the top quark rest frame and the lepton direction in the W boson rest frame.*

6.3 Top Quark Polarization

The goal of this analysis is to estimate the sensitivity of ATLAS to the measurement of the polarization of the top quarks produced by the Wg single top quark process.

Since the top quark is massive, it is not obvious that using the top quark direction of motion in the rest frame of the incoming partons as the polarization axis (the helicity basis) is the optimum basis in which to perform the polarization measurement. Recent theoretical work [23] has shown that the top quark spin direction is 100% correlated with the direction of the d-type quark for single top quark events in Wg events. In the vast majority of boson-gluon fusion events the d-type quark is the spectator quark responsible for producing a forward jet in these events. At the Tevatron [23] and LHC [24] this "spectator" basis has been shown to be the optimum basis in which to measure the top quark polarization. Since the sample used in this measurement contains only events with two jets, it is possible to assume that the spectator quark and the top quark are back-to-back in the center-of-mass frame of the incoming partons. Therefore, the spectator and

helicity bases are equivalent for this event sample. The measurement is treated here as if it were performed in the helicity basis.

Method of Measurement

The experimental measurement of the polarization of the top quark will essentially be a measurement of the angular distribution of its decay products in the top quark rest frame. The most sensitive angle is the one between the top quark direction in the zero momentum frame (center-of-mass frame of the incoming partons) and the direction of the charged lepton from the top quark decay in the top quark rest frame. This angle (θ_l) is illustrated in Figure 4. In the absence of background or detector effects the angular distribution of the charged lepton is given by

$$f(\cos\theta_l) = \frac{1}{2}(1 - P\cos\theta_l) \tag{1}$$

where P is the polarization of the sample and can range from -1 to 1. The convention chosen in this analysis is that 100% left-polarized top quarks have P=+1. The top quark polarization predicted by the Standard Model depends on the flavor of the light quark appearing in the initial state. The value associated with the parton density functions used in this study (CTEQ2L [25]) is P=+94.6%, which corresponds to a fraction of left handed top quarks of approximately 97% [26].

Experimentally, in order to measure the angular distribution of the charged lepton it is necessary to first reconstruct the momentum of the top quark in the rest frame of the initial state partons. In the case of Wg events this means adding the reconstructed 4-momenta of the top quark and the spectator quark jet in order to reconstruct the initial frame. However, the reconstruction of the top quark 4-momentum suffers from the ambiguity in the reconstruction of the z-momentum of the neutrino produced in the top quark decay (as described in Section 4). Once the top quark 4-vector in the rest frame of the initial state partons has been obtained, it can be used in the top quark rest frame since it is not rotated by a boost along its 3-vector direction. This allows it to be compared to the direction of the lepton in the top quark rest frame in order to measure the angle θ_l.

In order to illustrate the extraction of the value of the top quark polarization from the angular distribution, reference event samples were created with 100% left-polarized top quarks and 100% right-polarized top quarks. These reference distributions were compared to a statistically independent data set with the predicted Standard Model top quark polarization. This comparison was done by minimizing

$$\chi^2 = \sum_{\cos\theta_i} \frac{(f_{\rm th}(\cos\theta_l)_i - f_{\rm d}(\cos\theta_l)_i)^2}{\sigma^2_{{\rm th}_i} + \sigma^2_{{\rm d}_i}} \tag{2}$$

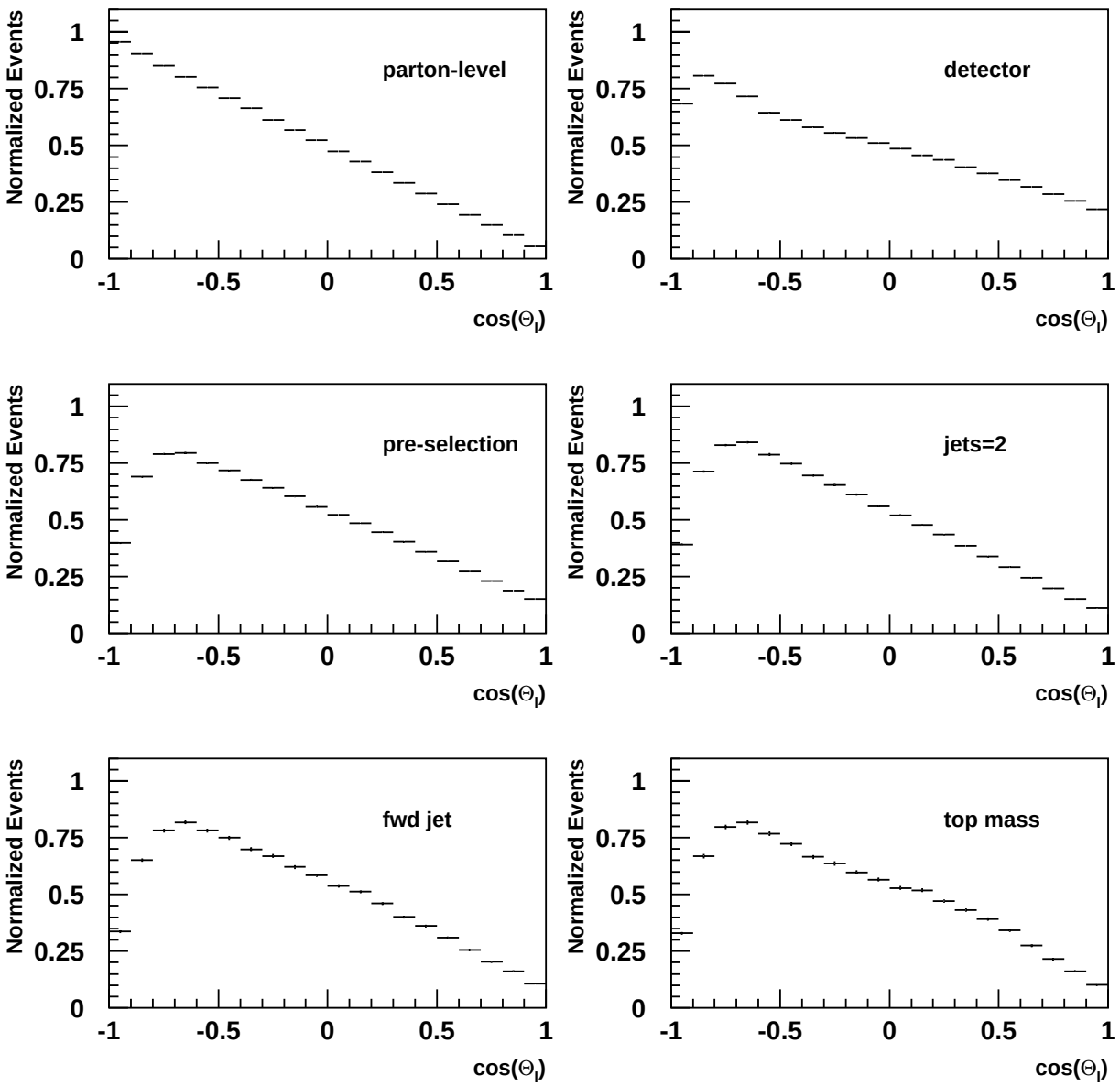

Figure 5: *Angular distribution of charged lepton in top quark rest frame for various data samples. The histograms progress from left-to-right, top-to-bottom. The first histogram shows the parton-level distribution. The second histogram is after the simulation of detector and reconstruction effects. The final 4 histograms illustrate the influence of event selection criteria on the angular distribution. The effects of the cuts are cumulative and are the result of adding pre-selection cuts, a jet multiplicity requirement, a forward jet tag and a top quark mass window respectively.*

where the subscript d represents quantities calculated for the data distribution and the subscript th refers to the generated reference distribution.The theoretical value $f_{\rm th}(\cos\theta_l)$ is calculated via

$$f_{\rm th}(\cos\theta_l) = \frac{1}{2}((1+P)f_L(\cos\theta_l) + (1-P)f_R(\cos\theta_l)) \quad (3)$$

where f_L and f_R refer to the value of the generated theoretical distribution for the 100% left-polarized and the 100% right-polarized top quarks respectively and P is the polarization of the top quark sample. The procedure returns an estimate of the top quark polarization and an error on that estimate. In this way the sensitivity to changes in top quark polarization can be quantified.

Effects of Detector and Event Selection

Moving from the parton-level simulation to a simulation which includes radiation, hadronization and detector effects is certain to complicate the measurement of the polarization of the top quark. In addition, the signal could be biased by an event selection designed to eliminate background and will be contaminated by residual background events.

The first histogram in Figure 5 shows the parton-level angular distribution for a sample of Wg fusion events with a SM polarization. The second histogram in Figure 5 shows the angular distribution of the charged lepton after detector effects have been simulated. In addition to effects associated with detector energy smearing, jet and cluster definitions, etc. this distribution includes the effects of ambiguities in reconstructing the top quark due to the absence of information about the neutrino z-momentum. It does not, however, contain the effects of any event selection in order to separate signal from background. This histogram demonstrates that the effect of radiation, hadronization and detector resolution changes the shape of the angular distribution but still produces a highly asymmetric distribution.

In addition to the effects introduced by the detector resolution, the effect of applying the event selection criteria described in Section 4 can be evaluated by applying them one at a time and observing the change in shape of this distribution. This set of criteria leads to an overall signal efficiency of 3.0%, resulting in more than 16000 events in one year of low-luminosity data-taking at ATLAS ($1 \times 10^4 \mathrm{pb}^{-1}$). Figure 5 demonstrates the effect of applying these cuts in a cumulative manner. Again the asymmetry of the angular distribution is preserved, though more degradation is clearly evident, in particular near $\cos\theta_l = -1$. The degradation is worse at these values of $\cos\theta_l$ because the leptons from these events are emitted in the direction opposite to the top quark boost. This reduces the momentum of the leptons causing more of them to fail p_T-based selection criteria.

Since W+jets events dominate the background remaining after cuts, it is treated as the only background in this analysis. Figure 6 shows the cumulative effect of cuts on the

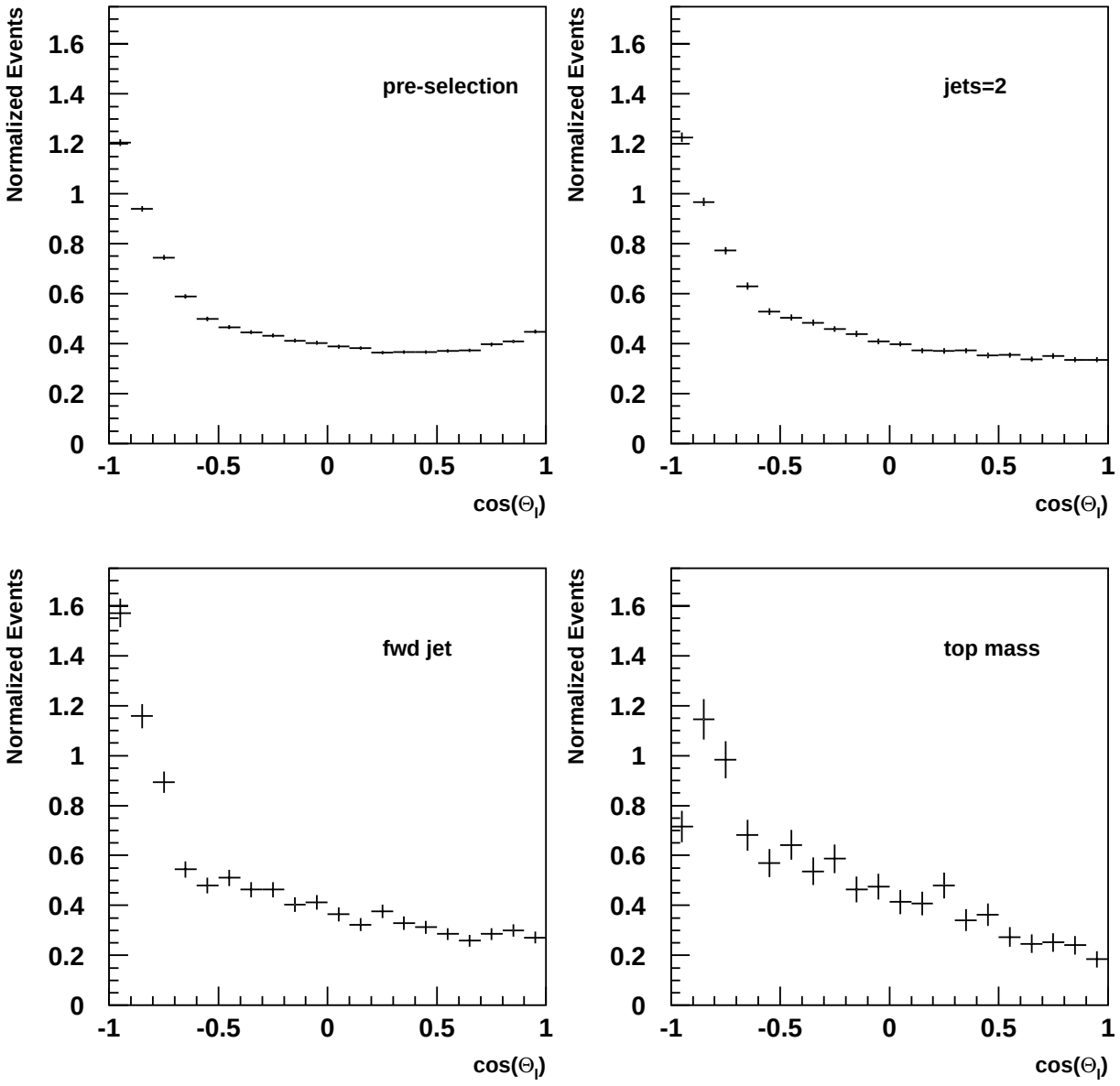

Figure 6: *The effect of event selection cuts on the angular distribution of the charged lepton in W+jets events. The effects of the cuts are cumulative. The first distribution is the result of applying the pre-selection (trigger) cuts only and cuts are applied cumulatively from left-to-right, top-to-bottom.*

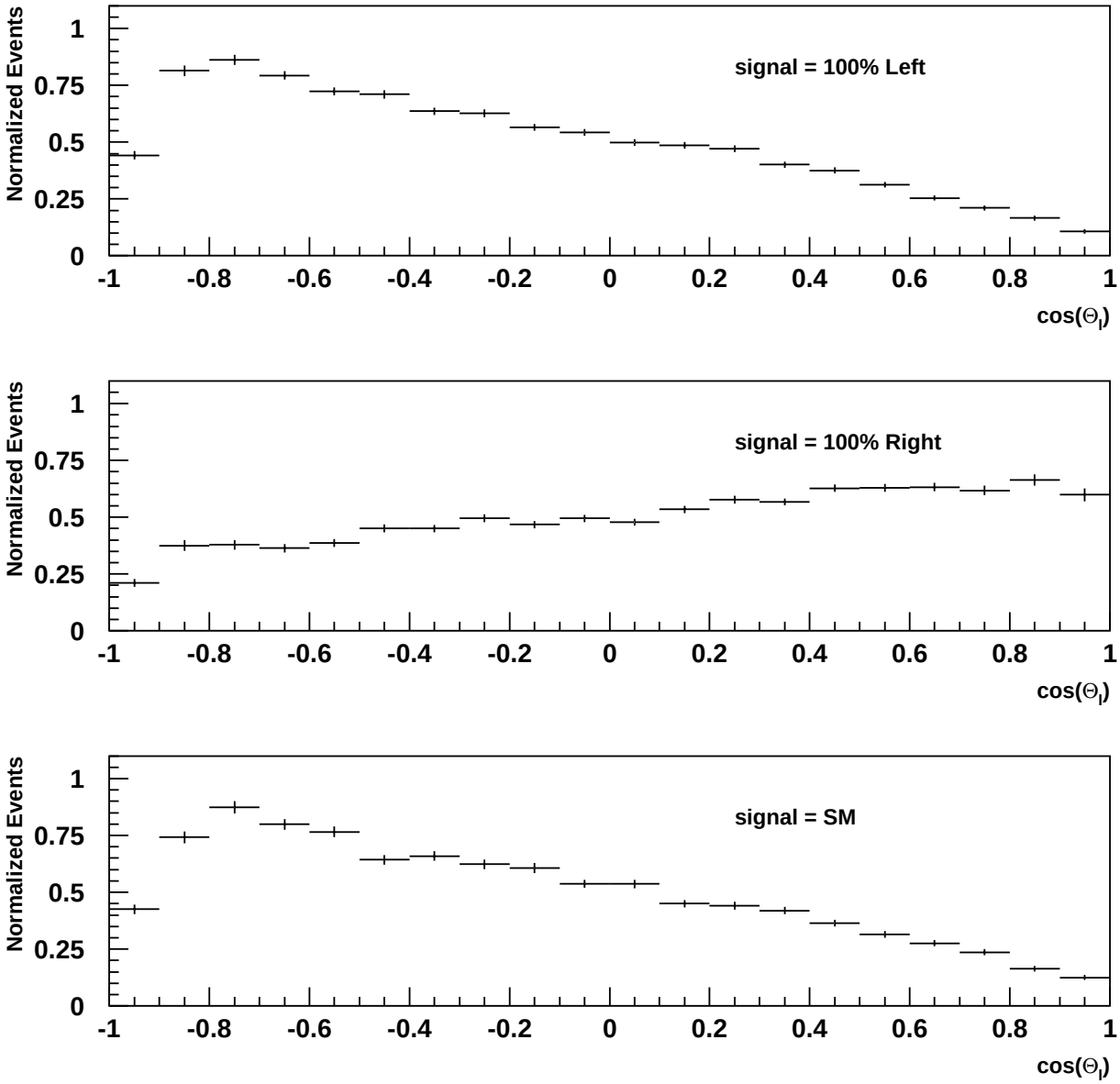

Figure 7: *The first histogram shows the reference distribution for 100% left-handed top quarks after detector effects and event selection criteria have been applied and the appropriate level of background has been mixed in. The second histogram shows the reference distribution for 100% right-handed top quarks. The third histogram represents the expected Standard Model distribution for a statistically independent sample of signal and background.*

angular distribution of the charged lepton from W+jets events. A peculiar feature of these events is evident in all of these distributions. This is the tendency for events to be grouped near $\cos\theta_l = -1$. The events which populate this region tend to be the highest p_T events. This shows that even basic jet and isolated lepton definitions and pre-selection cuts bias the angular distribution of W+jets events.

Results

When the event selection criteria described in Section 4 are applied, the signal-to-background ratio (treating W+jets as the only background) is found to be 2.6. Using the methods described earlier it is possible to estimate the polarization of a mixed sample of Wg signal and W+jets background. The reference distributions for 100% left and right-polarized top quarks mixed with background in a ratio of 2.6:1 are shown in Figure 7. Also shown is the angular distribution corresponding to a statistically independent data sample with Standard Model polarization mixed with background in the ratio 2.6:1.

The chi-squared function presented in Equation 2 is minimized in order to obtain an estimate of the polarization of the top quark. To estimate the precision for one year of data-taking at ATLAS, the fit was done with 3456 signal events and 1345 background events corresponding to 0.2×10^4 pb^{-1} of integrated luminosity at ATLAS ($\sim 1/5$ of a year). For this integrated luminosity the value of the polarization is found to be 95.8% with an error of 4.0%. The systematic error associated with a $\pm 20\%$ variation of the background level contributes an additional 0.5%. This result is in good agreement with the parton-level prediction of 94.6%.

Assuming the statistics on the reference distributions, $f_L(\cos\theta_l)$ and $f_R(\cos\theta_l)$, will lead to a negligible source of error at ATLAS, this precision improves to 3.5%. Projecting these results to one year of data-taking at low luminosity (1×10^4 pb^{-1}), assuming the errors scale as the square root of the number of events, yields a predicted precision of 1.6% on the measurement of the top quark polarization after one year of data-taking at ATLAS.

6.4 W Boson Helicity Measurement

W boson polarization depends on the properties of the W-t-b vertex present in top quark decay. New physics, such as the existence of V+A couplings at the W-t-b vertex, could alter the predictions of the SM concerning the polarization of W bosons produced in top quark decays. This section presents an estimation of the expected sensitivity of ATLAS to the polarization state of the W boson boson produced in top quark decays via Wg fusion. The sensitivity to non SM contributions is also explored.

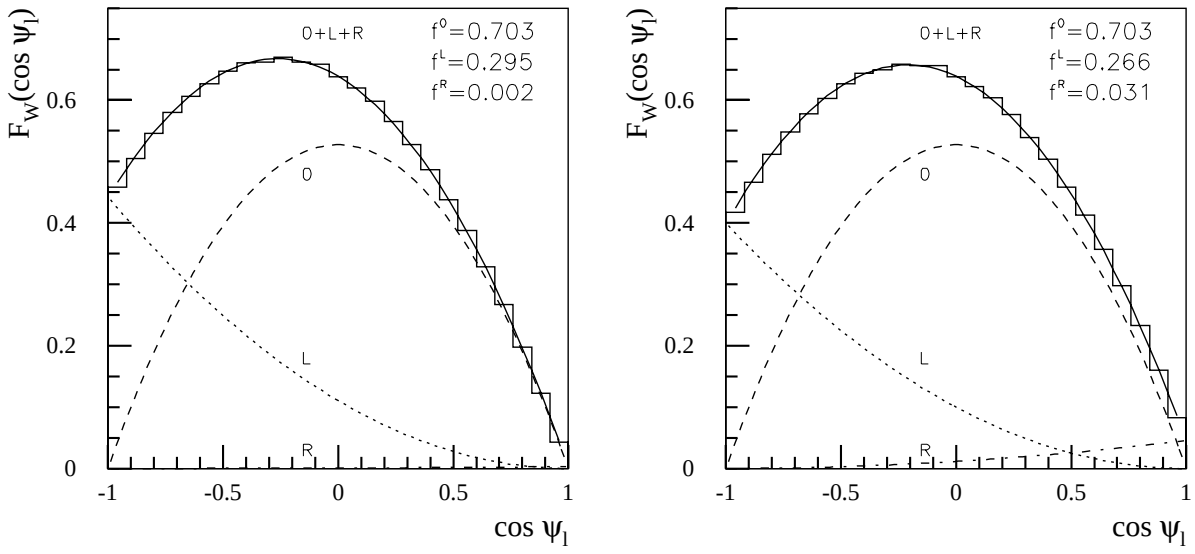

Figure 8: *Parton level distributions of the cosine of the lepton angle in the W boson rest frame for the SM scenario with $f_R = 0$ (left) and an alternative scenario in which there is a 3% right handed component included at the expense of the left handed fraction. The curves correspond to a "SM-like" fit ($f_{long} = 0.703$, $f_L + f_R = 0.297$) resulting in $f_R = 0.002$ (left) and $f_R = 0.031$ (right). In each figure, the predicted contributions from longitudinal (0), left-handed (L) and right-handed (R) polarizations are shown separately, as well as their sum.*

Method of Measurement

The polarization of the W-boson can be determined by measuring the angular distribution of the charged lepton in the rest frame of the W, $\cos\psi_l$. A diagram of ψ_l is shown in Figure 4. Fortunately, it is not necessary to reconstruct the W boson rest frame in order to obtain this angular distribution. Instead, it is possible to reconstruct $\cos\psi_l$ in terms of the invariant mass of the lepton and the b produced in top quark decay [27]:

$$\cos\psi_l = \frac{2 \cdot M_{lb}^2}{M_t^2 - M_W^2} - 1 \tag{4}$$

The distortion introduced by the ambiguity in the reconstruction of the z component of the neutrino momentum is eliminated when using this method.

The angular distribution in the W boson rest frame is described by:

$$F_W(\cos\psi_l) = \frac{3}{2} \cdot \left[f_{long} \cdot \left(\frac{\sin\psi_l}{\sqrt{2}} \right)^2 + f_L \cdot \left(\frac{1-\cos\psi_l}{2} \right)^2 + f_R \cdot \left(\frac{1+\cos\psi_l}{2} \right)^2 \right] \tag{5}$$

where f_{long}, f_L and f_R are the fractions of longitudinal, left and right-handed polarized W bosons. In the SM the W boson from top quark decay can only be longitudinally or

left handed polarized, (f_R=0), and the ratio of longitudinal to left-handed W bosons is predicted to be:

$$\frac{f_{long}}{f_L} = \frac{M_t^2}{2 \cdot M_W^2} \tag{6}$$

For a top quark with $M_t = 175$ GeV this prediction yields $f_{long} = 0.703$ and $f_L = 0.297$. The contribution to the W boson polarization from each component can be extracted from a fit to the measured distribution of $\cos\psi_l$, according to (5).

In order to explore the sensitivity to non-SM contributions, events with right-handed W boson polarization were introduced in the simulation by treating the neutrino in SM events as a charged lepton, and vice-versa. In addition to a sample of events simulated with the SM prediction, a "SM-like" scenario, in which the non-longitudinal fraction $1 - f_{long} = 0.297$ is shared by f_L and f_R, was simulated. Figure 8 shows the distribution of $\cos\psi_l$ at parton level, for the SM scenario, and for a more general situation with $f_{long} = f_{long}^{SM} = 0.703$, $f_L = 0.90 \times f_L^{SM} = 0.267$ and $f_R = f_L^{SM} - f_L = 0.030$.

Several functions were used to to fit the $\cos\psi_l$ distributions, including a pure SM fit which assumes $f_R = 0$, a "SM-like" fit with f_{long} fixed to the SM value and the fraction f_L being returned ($f_R = 1 - f_{long}^{SM} - f_L$), and a more general fit in which the only constraint was $f_{long} + f_L + f_R = 1$. The results obtained with the SM sample yielded values for f_{long}, f_L and f_R which differed by less than 1.5% from the generated values. When using the mixed sample in which $f_R = 0.10 \times f_L^{SM} = 0.030$, the "SM-like" and the more general fit both returned non-zero values of 10.3% and 9.7% of f_L^{SM} respectively. The "SM-like" fit results are shown in Figure 8. In the non SM- scenario, a pure SM fit, under the hypothesis of a zero f_R is clearly disfavoured, with a χ^2 per degree of freedom of 40-50 times higher than obtained with the fits with f_R as a free parameter.

Effects of Detector and Event Selection

Several factors could potentially affect the shape of the distribution of $\cos\psi_l$. In addition to the modifications originated by radiation, the distribution could be biased by the detector acceptance, event selection and residual background contamination. The following figures illustrate the influence of this factors.

Figure 9 presents the evolution of the angular distribution through the selection process for a sample of Wg signal. The differences between parton level and detector histograms are due to radiation, hadronization and detector effects. The second distribution also includes other effects related with the reconstruction of the top quark kinematics, such as the reconstruction of the neutrino momentum, or the minimum requirement of having at least one lepton, one b-jet and an additional jet. The radiation is responsible for a spreading of the distribution leading to a non-zero value at $\cos\psi_l = 1$. The trigger selection (see Section 4) is responsible for an important distortion on the negative values of $\cos\psi_l$, as

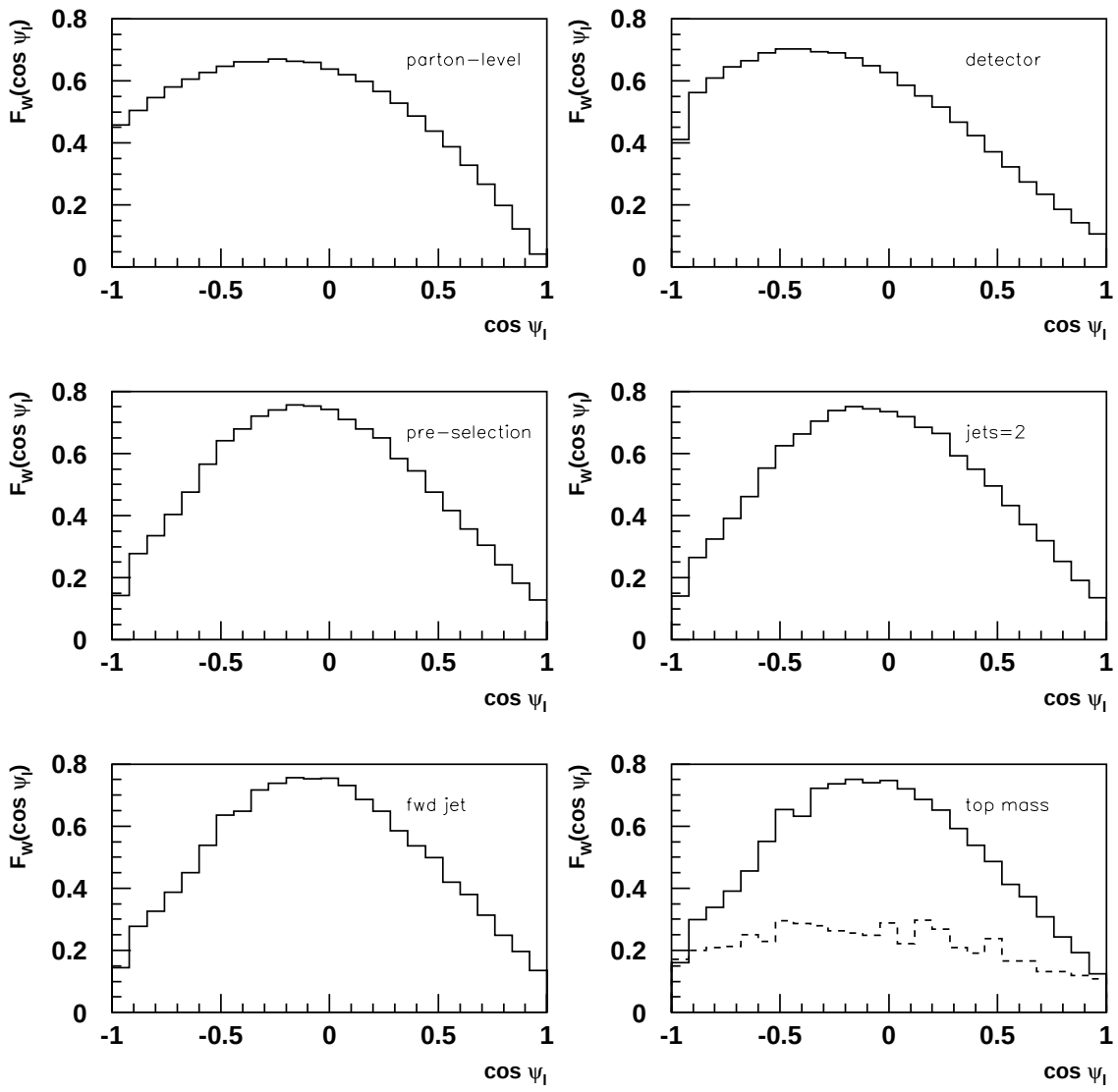

Figure 9: *Angular distribution of the charged lepton in the W boson rest frame for a sample of Wg fusion events. The histograms progress from left-to-right, top-to-bottom. The first histogram shows the parton-level distribution. The second histogram includes radiation and hadronization, the simulation of detector and reconstruction effects. The final 4 histograms illustrate the influence of event selection criteria on the angular distribution. The effects of the cuts are cumulative and are the result of adding pre-selection cuts, a jet multiplicity requirement, a forward jet tag and a top quark mass window respectively. The dotted histogram in the last figure corresponds to the contribution of the W+jets background.*

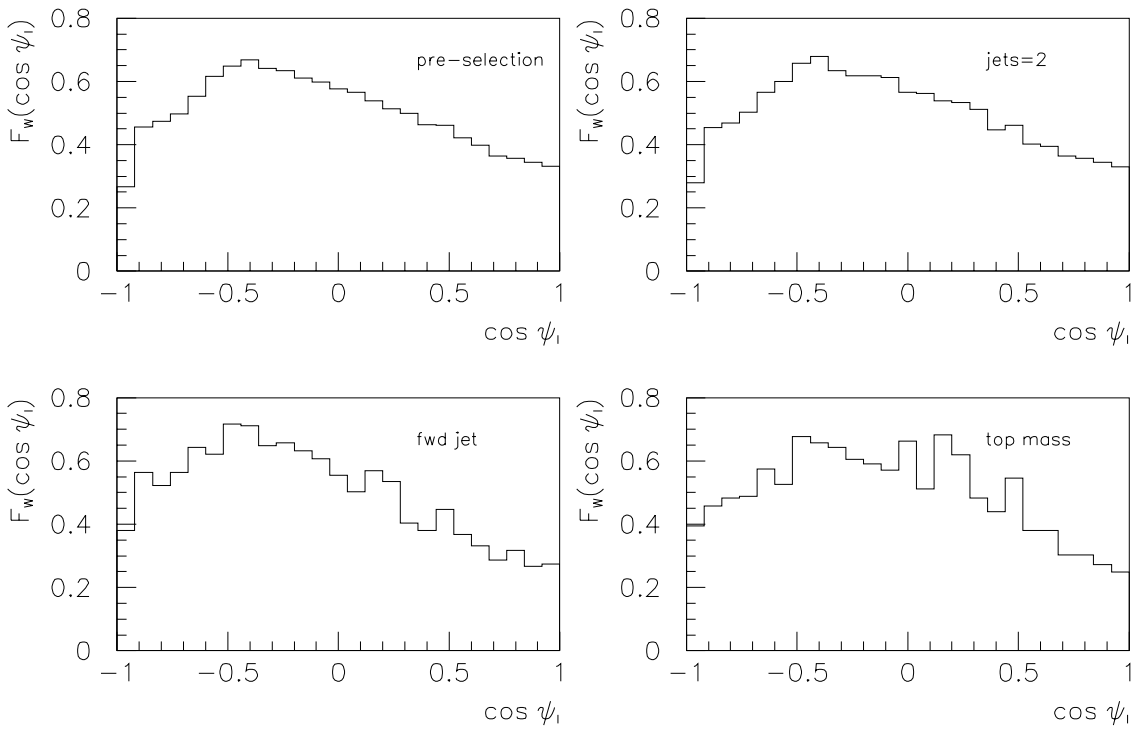

Figure 10: *The effect of event selection cuts on the angular distribution of the charged lepton in W+jets events. The effects of the cuts are cumulative. The first distribution is the result of applying the pre-selection (trigger) cuts only and cuts are applied cumulatively from left-to-right,top-to-bottom.*

shown in the third histogram. This is mainly due to the minimum p_T requirement for leptons. This part of the distribution is populated by leptons emitted against the direction of the W boson boost, which consequently have a reduced momentum. The remaining selection criteria defined in Section 4, don't introduce further distortion, as shown in the last distributions of Figure 9. The relative contribution of the W+jets background, assuming a signal-to-background ratio of 2.6 has been superposed to the last figure.

W+jets is treated as the only background as done previously in the study of the top quark polarization. Figure 10 shows the effect of the selection criteria on the angular distribution of the charged lepton in W+jets events. A bias of the background distribution is introduced with the reconstruction of a "$\cos\psi_l$" from a lepton, b-jet and jet in W+jets events. The shape of the distribution remains stable through additional event selection. Two statistically independent distributions in agreement with the shape and amount of background expected in three years after event selection were produced in order to fake the effect of background addition and subtraction.

An acceptance/efficiency correction was applied to the distribution after event selection

in order to recover, at least partially, the original shape. The correction was obtained from a fit to the distribution of the ratio between the distributions after selection and at parton level. In order to simulate a strategy for making a precision measurement,a cut was employed on the measured $\cos\psi_l$ distribution. This cut restricts attention to the region in which the correction is slowly varying (acceptance/efficiency > 0.02, so $\cos\psi_l > -0.6$) and which avoids anomalous behaviour related to radiation ($\cos\psi_l < 0.8$). The resulting function is shown in Figure 11.

Results

The final distribution of $\cos\psi_l$ obtained from a sample of signal and background corresponding to $3 \times 10^4 \mathrm{pb}^{-1}$combined in a ratio 1:2.6 after event selection, efficiency correction and background subtraction is shown in Figure 11. The errors include the statistics due to background subtraction. The polarization was extracted from a fit in the restricted region under the single constraint $f_{long} + f_L + f_R = 1$ resulting in $f_{long} = 0.705 \pm 0.015$, $f_L = 0.293 \pm 0.010$ and $f_R = 0.002 \pm 0.018$. This result is compatible with the initial hypothesis of a SM sample with a zero right handed component. The values obtained for the longitudinal and right handed components differ by less than 2% from the expected values.

The influence of a 20% uncertainty in the calculation of the background rate has been estimated by modifying the amount of background in the sample by $\pm 20\%$ while still assuming the predicted rate (see Table 1). The systematic errors associated with the sensitivity to the background level are $\epsilon(f_{long})/f_{long} = \pm 0.6\%$ and $\epsilon(f_L)/f_L = \mp 1.0\%$.

7 Conclusions

The analyses presented in this note have been performed with a simple set of selection criteria leading to a reasonable compromise between signal-to-background ratio and signal efficiency. The signal to background ratio could benefit from a tighter selection, but at the cost of signal efficiency which would yield no benefit in the V_{tb} measurement.

The fractional statistical error obtained in the measurement of V_{tb} is 0.27%. Without considering systematic errors arising from detector effects, the dominant source of error is likely to be the uncertainty in the parton distribution functions, which contribute at the level of 5%. The combination of theoretical and statistical errors yields $\Delta V_{\mathrm{tb}}/V_{\mathrm{tb}}$=5.5%.

Top quark and W boson polarization measurements have been performed by studying the angular distributions of the charged lepton in their respective rest frames. A different method was used in each case in order to simulate the effect of non-Standard-Model contributions. In the case of the top quark, a weighting procedure was used to generate

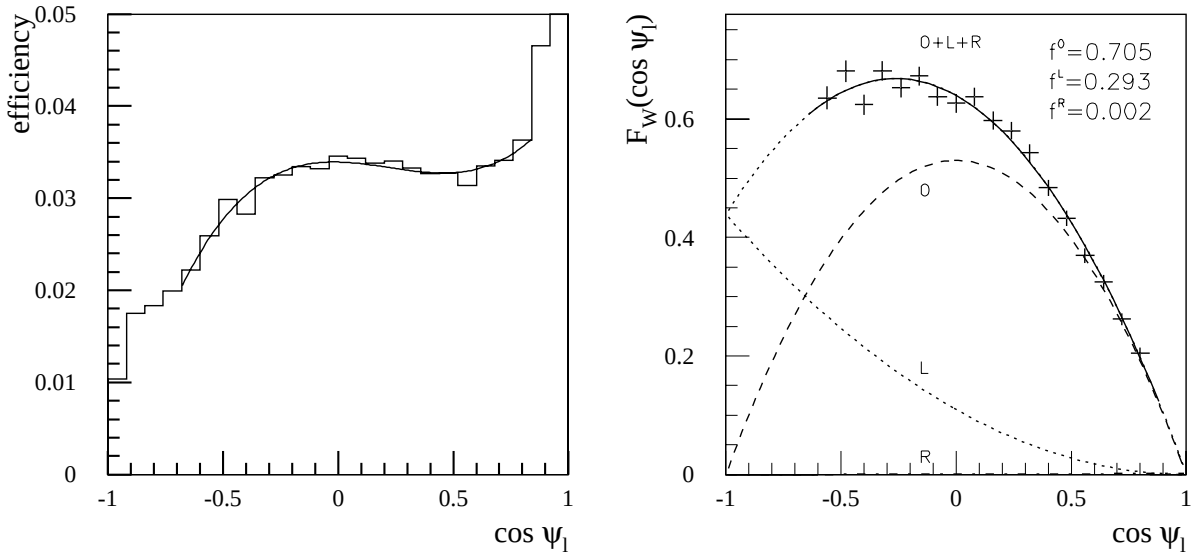

Figure 11: *Left: Ratio between the distribution of* $\cos\psi_l$ *at parton level and after selection criteria have been applied. The function resulting from the fit (solid line) has been used to correct the distribution of selected events. Right: Distribution of the cosine of the lepton angle in the W boson rest frame after selection, efficiency correction and background subtraction. The solid curve corresponds to a fit in agreement with (5) in which the three components are bounded by* $f_{long} + f_L + f_R = 1$*. The resulting contributions from longitudinal (0), left-handed (L) and right-handed (R) polarizations, extended to the full range of* $\cos\psi_l$*, are shown separately, as well as their sum.*

theoretical distributions for 100% left-handed and 100% right-handed top quark samples. In order to perform the W boson polarization measurement right-handed bosons were introduced by exchanging the neutrino and the electron produced in its decay. The top quark polarization after one year of data-taking at low luminosity ($1 \times 10^4 \mathrm{pb}^{-1}$) is founded to be 95.8% with an error of 1.6%. The contributions to the W boson polarization corresponding to a luminosity of $3 \times 10^4 \mathrm{pb}^{-1}$ were founded to be $f_{long} = 70.5 \pm 1.5\%$ and $f_L = 29.3 \pm 1.0\%$, which results in a right component compatible with a zero value, as expected in the Standard Model.

Acknowledgements

We would like to thank G. Mahlon, S. Mrenna, S. Parke, T. Tait, S. Willenbrock and C.P. Yuan for many valuable discussions on top quark physics. We are also grateful to M. Cobal, J. Jean, R. Mehdiyev, J. Parsons, S. Slabospitsky and J. Womersley for helpful interactions during this analysis, which have contribute to improve the results presented in this note.

References

[1] Willenbrock, S., "Top Quark Physics for Beautiful and Charming Physicists". hep-ph/9709355, Sep. 1997.

[2] Particle Data Group, "Review of Particle Physics". *European Physical Journal* C3:1-794, 1998.

[3] Konigsberg, J., "Top and Higgs at the Tevatron: Measurements, Searches, Prospects", Fermilab-Conf-99/129E, Published Proceeding, 17th International Workshop on Weak Interactions and Neutrinos (WIN 99), Cape Town, South Africa, 1999.

[4] *ATLAS Detector and Physics Performance Technical Design Report*, Volumes I and II CERN/LHCC/99-14 and CERN/LHCC/99-15, May 1999.

[5] Lagatta A., Simak V. and Smolik J., "$t\bar{t}$ spin correlations and and the potential for observation of CP violation in the production vertex, ATL-COM-PHYS-99-049.

[6] Stelzer, T., Sullivan, Z., Willenbrock, S., "Single-Top-Quark Production via W-Gluon Fusion at Next-to-Leading Order". Physical Review D56:5919-5927, 1997.

[7] Smith, M. and Willenbrock, S., "QCD and Yukawa corrections to single top production via $q\overline{q} \to t\overline{b}$". Physical Review D, Volume 54, page 6696, 1996.

[8] Bonciani, R., Catani, S., Mangano, M. and Nason, P., "NLL Resumation of the Heavy-Quark Hadroproduction Cross-Section". Nuclear Physics B. 529:424-450, 1998.

[9] Seltzer, T., Sullivan, Z. and Willenbrock, S., "Single-top-quark Production at Hadron Colliders". hep-ph/9807340, July 1998.

[10] G. Marchesini, B.R. Webber, G. Abbiendi, I.G. Knowles, M.H. Seymour and L. Stanco, " A Monte Carlo Event Generator for Simulating Hadron Emission Reactions with Interfering Gluons", Computer Phys. Commun. 67(1992) 465.

[11] Berends, F.A., Kuijf, H., Tausk, B. and Giele,W.T., "On the Production of a W and Jets at Hadron Colliders", Nucl. Phys. B 357:32-64,1991.

[12] Mangano, M., "Production of W Plus Heavy Quark Pairs in Hadronic Collisions" Nuclear Physics, v.405 page 536 (1993).

[13] D. O'Neil, B. González Piñeiro and M. Lefebvre, "Measuring $V_{\rm tb}$via s-channel Single Top at ATLAS", ATL-PHYS-99-011.

[14] Tait, T. and Yuan, C.P., "The Phenomenology of Single Top Quark Production at the Fermilab Tevatron", hep-ph/9710372, Oct. 1997.

[15] Tait, T., private communication and Huston, J. et al. "Study of the Uncertainty of the Gluon Distribution", hep-ph/9801444, Jan. 1998.

[16] Willenbrock, S., "Overview of Single Top Theory - Measuring the Cross-section, Theoretical Uncertainties, $|V_{\rm tb}|$, etc.", Talk presented at the "Thinkshop, Top-Quark Physics for Run II" at Fermi National Laboratory, Bhatavia, Illinois, October 16-18th, 1998.

[17] D.O. Carlson, "Physics of Single Top Production at Hadron Collider", Michigan State U. Ph.D. Thesis, UMI-96-05840-mc (microfiche), 1995. 126pp. S. Mrenna, T. Tait, and C.-P. Yuan, private communication.

[18] Sjostrand, T., "High-Energy Physics Event Generation with PYTHIA 5.7 and JETSET 7.4", Computer Physics Communications 82 (1994) 74.

[19] Richter-Was, E., Froidevaux, D., Poggioli, L., "ATLFAST 2.0 a fast simulation package for ATLAS", ATLAS Internal Note: ATL-PHYS-98-131.

[20] O'Neil, D., "The Physics of Electroweak Top Quark Production at ATLAS", University of Victoria Ph.D. thesis, 1999.

[21] A. Ahmedov et al., "Single Top Quark Production via W-Gluon Fusion at LHC, simulation with PYTHIA 5.7 Event Generator", ATLAS Note: ATL-COM-PHYS-99-076.

[22] Guillian, G., Campbell, M. and Amidei, D., "The Choice of Measurements for Studying the Top Quark Decay Product Angular Distribution",CDFNOTE 4262, Oct. 1997.

[23] Mahlon, G. and Parke, S., "Improved Spin Basis for Angular Correlation Studies in Single Top Production at the Fermilab Tevatron", *Physical Review* D55:7249-7254, 1997.

[24] Mahlon, G. and Parke, S., "Single Top Quark Production at the LHC: Understanding Spin", hep-ph/9912458, Dec. 1999.

[25] Tung, W., "Perspectives on Global QCD Analyses", Proceedings of the International Workshop on Deep Inelastic Scattering and Related Subjects, Eilat, Israel (1994), ed. Levy, A., World Scientific Publishing Co., Singapore.

[26] Tait, T., "Signals for the Electroweak Symmetry Breaking Associated with the top quark", Michigan State University Ph. D. thesis, 1999.

[27] Kane, G. L., Ladinsky, G. A., Yuan, C. P., "Using the top quark for testing standard-model polarization and CP predictions", Phys. Rev. D 45, (1992) 124.